

# Calibration of the LIGO detectors for the First LIGO Science Run

**Rana Adhikari<sup>1</sup>, Gabriela González<sup>2</sup>, Michael Landry<sup>3</sup> and Brian O'Reilly<sup>4</sup> (for the LIGO Scientific Collaboration)**

<sup>1</sup> Department of Physics and Center for Space Research, Massachusetts Institute of Technology, Cambridge, MA 02139, USA

<sup>2</sup> Department of Physics and Astronomy, Louisiana State University, 202 Nicholson Hall, Baton Rouge, LA 70803, USA

<sup>3</sup> LIGO Hanford Observatory, PO Box 159, Richland, WA 99352, USA

<sup>4</sup> LIGO Livingston Laboratory, PO Box 940, Livingston, LA 70754, USA

E-mail: gonzalez@lsu.edu

Received 29 April 2003

Published 18 August 2003

Online at [stacks.iop.org/CQG/20/S903](http://stacks.iop.org/CQG/20/S903)

## Abstract

We describe the calibration procedures applied to the data taken by the three LIGO interferometric gravitational wave detectors in the LIGO Science Collaborations First Science Run, from 23 August to 9 September 2002. The calibration depends on corrections to feedback servos used in the instrument, and on changing optical gains. We describe the stability of the calibration and detector sensitivity during the 17-day run.

PACS numbers: 04.80.Nn, 95.55.Ym, 95.75.Wx

(Some figures in this article are in colour only in the electronic version)

## 1. Introduction

The Laser Interferometer Gravitational-Wave Observatory (LIGO) is an ambitious US initiative to detect gravitational waves from astrophysical sources such as coalescing neutron stars and black holes, spinning neutron stars, and supernovae. The LIGO interferometers [1, 2] form part of a worldwide network of gravitational-wave detectors which includes the British–German GEO detector [3], the French–Italian VIRGO detector [4] and the Japanese TAMA detector [5].

The LIGO detectors are laser interferometers with light propagating between large suspended mirrors in two perpendicular arms. They measure the strain (differential fractional change in arm lengths) produced by gravitational waves from astrophysical sources by monitoring the relative optical phase between light paths in each arm [6]. LIGO comprises

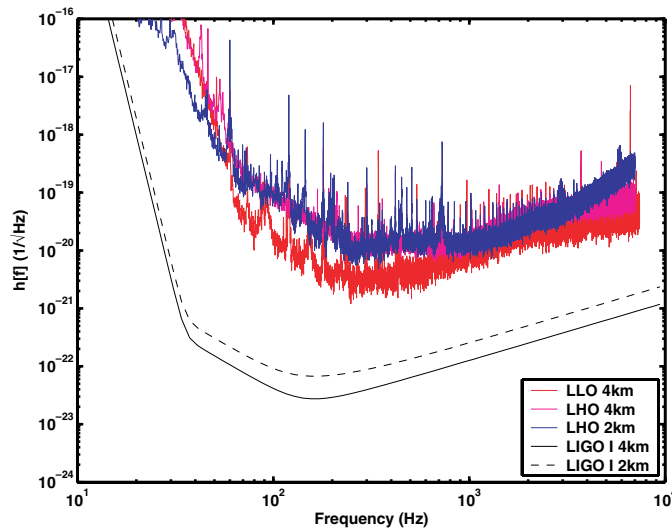


**Figure 1.** Typical sensitivities of the three LIGO interferometers during the S1 data run, shown as equivalent strain amplitude spectral density  $h(f)$ . These amplitudes were obtained using the calibrations described in this paper.

three detectors housed at two geographically separated locations: in Hanford, WA, there are two interferometers, one with arms 4 km long (which is referred to as H1 in this paper) and one with arms 2 km long (H2), while in Livingston, LA, there is one interferometer with arms 4 km long (L1) [2].

The First LIGO Science Run, S1, lasted from 23 August 2002 to 9 September 2002. Figure 1 shows amplitude spectra of equivalent strain noise, typical of the three LIGO interferometers during the S1 run. The strain noise design goal is also indicated for comparison. The differences between the three spectra reflect differences in the operating parameters and hardware implementations of the three instruments; they are in various stages of reaching the final designed configuration. The 17-day run yielded 363 h of data when at least one interferometer was in stable operation. The three interferometers were operating simultaneously for 95.7 h.

The calibration of the interferometric signal interpreted as strain is an essential element of the data analysis. We start with a simple model of the interferometer, measurements of different parts of the model and the interpretation of the observed amplitude of calibration lines as model parameters. We describe in this paper the procedures used in the LIGO detectors for the S1 run and the results obtained in terms of stability of the detectors during the run<sup>5</sup>.

## 2. A simple model of the detector

Each arm of the LIGO detectors contains two test masses, a partially transmitting mirror near the beam splitter and a near-perfect reflector at the end of the arm. Each such pair is oriented to form a resonant Fabry–Perot cavity with a gain buildup factor of 140 (corresponding to a cavity pole at  $\simeq 90$  Hz) which further increases the strain induced phase shifts by a factor

<sup>5</sup> More details and a careful estimate of errors associated with calibration of the LIGO detectors during S1 can be found in the LIGO Technical Document T030097-00-D, available in <http://admbdbsrv.ligo.caltech.edu/dcc/>.

proportional to the cavity finesse. The light from the two arm cavities interferes at the central beamsplitter, producing the gravitational wave signal at the ‘dark port’. The light reflected by the interferometer is used by a power recycling cavity, resulting in a smaller shot noise limitation to the detector sensitivity. Various feedback control systems are used to keep the multiple optical cavities tightly on resonance [7] and well aligned [8].

A gravitational wave would produce a signal of amplitude  $h(t) = (L_x(t) - L_y(t))/L_0$  if the distances were only changed by gravitational waves; however many other sources of noise (in displacement and in sensing) add to the sensed signal  $s(t)$ . The actual strain signal  $s(t)$  is derived from the error signal  $e(t)$  of the feedback loop used to control the differential motion of the interferometer arms. The calibration for LIGO in this science run was performed in the frequency domain, providing a response function  $R(f)$  that relates the Fourier transforms of the measured error signal  $e(f)$  and the interferometer signal  $s(f)$ :  $s(f) = R(f)e(f)$ . The interferometer signal is produced by the changes in difference of length between the two orthogonal interferometer arms, divided by the arm length:  $s(t) = (L_x(t) - L_y(t))/L_0$ .<sup>6</sup> The length  $L_0$  is 2 km for H2 and 4 km for H1 and L1. To understand how to estimate the response function from measurements of more fundamental components, we create a simple model of the sensing of the single degree of freedom corresponding to the differential arm signal. The response function can be built from three elements in the feedback loop: a sensing function  $C(f)$ , an actuation function  $A(f)$  and a digital compensation (feedback filter) function  $D(f)$ . We describe these functions in the following subsections.

### 2.1. Sensing function $C(f)$

The sensing function considered in this model,  $C(f)$ , converts the strain into the error signal registered by our data acquisition system. In the absence of a feedback loop, we have  $e(f) = C(f)h_{\text{ext}}(f)$ . The sensing function has units of counts/strain. The frequency dependence of the sensing function is determined mainly by the resonant optical cavity in each arm (assumed to be identical in this model), which is simply a real cavity pole in the Laplace domain. The gain of the cavity sensing function depends on the power in the cavity, which in turn depends on the alignment of the cavity mirrors. Since all the LIGO detectors had a limited alignment control at the time of the S1 run, the alignment changed significantly during the period of operation. For this reason, keeping track of the calibration as a function of time was a critical part of the data analysis of S1 data.

The actual sensing of the interferometric signal is achieved by converting a photocurrent at the dark port into a radio-frequency voltage which carries the fluctuations in length as sidebands of a  $\approx 25$  MHz modulation frequency [7]. The signal is demodulated, amplified, whitened (to minimize the contribution of digitization noise in the analogue-to-digital conversion), anti-aliased (a low pass filter to suppress errors due to finite sampling frequency of 16384 Hz) and converted into the digital signal  $e(t)$ . These operations have known frequency dependencies and gains, and remained unchanged during the S1 run.

### 2.2. Actuation function $A(f)$

The optical cavities are kept in resonance by actuating on the suspended mirrors at the end of the long arms by means of electromagnetic actuators. These are four magnets glued to

<sup>6</sup> Note that this differs from the normal definition of strain by a factor of two. We use this definition because it translates directly into gravitational wave amplitude  $h(t)$ .

the back of the mirrors, and four coils around the magnets, attached to the suspension frame. The feedback signals are currents in the coils that attract or repel the magnets on the mirror, causing it to move to the desired position. The same actuators are used to align the mirrors, and to damp their pendulum motions, but in this paper we are only concerned about the use of these actuators for controlling the length of the cavities.

The actuation function  $A(f)$  relates a digital control signal  $g(f)$  in counts, to the strain  $s_c(f)$  that would be produced in the detector, due to the control system:  $s_c(f) = -A(f)g(f)$ . (By convention, the control signal is assumed to add negatively to cancel the external strain.) The frequency dependence is mostly determined by the pendulum suspension. The digital control signal produces a force on the mirror, which relates to the displacement (and thus strain) by a function with a pair of complex poles at the pendulum frequency,  $f_p = 0.75$  Hz. Before being converted into a force, the digital control signal is first filtered with de-whitening (to minimize the contribution of digitization noise in the analogue-to-digital conversion), anti-imaging (to minimize the effects of finite sampling frequency) and ‘snubbing’ filters (smoothing filters to eliminate transients), then amplified and converted into a current, which produces the electromagnetic force on the mirrors. The filters used are well known and measured, and were not changed during S1. The gain of the actuation function is not expected to change during operation, and its measurement is critical to the calibration process. Several different ways devised to calibrate the function  $A(f)$  are described in section 3.

### 2.3. Digital feedback filter function $D(f)$

To keep the optical cavities resonant, there is a digital feedback control system that applies a filter  $D(f)$  which converts the error signal  $e(f)$  into a control signal  $g(f)$ , and sends it as actuation to the mirrors. The filters used in S1 were different in the three detectors, but they are well known, constructed from a few parameters registered in the LIGO records. In a few instances during S1 these parameters changed but their values at any given time are known.

### 2.4. Response function $D(f)$

The closed loop system can be described with a few simple equations. We assume that a strain disturbance  $s(f)$  (due to the sum of gravitational waves, noise sources, and intended excitations such as a calibration line) is added to the effect of the control signal  $s_c(f) = -A(f)g(f)$ , producing a net, or residual, strain

$$s_{\text{res}}(f) = s(f) + s_c(f).$$

This net strain produces an error signal  $e(f) = C(f)s_{\text{res}}(f)$ , and this error signal is in turn converted into the control signal  $g(f) = D(f)e(f) = D(f)C(f)s_{\text{res}}(f)$ , so we have

$$s_{\text{res}}(f) = s(f) - A(f)D(f)C(f)s_{\text{res}}(f)$$

or

$$s_{\text{res}}(f) = \frac{s(f)}{1 + A(f)D(f)C(f)} = \frac{s(f)}{1 + G(f)}.$$

The function  $G(f) = A(f)D(f)C(f)$  is the *open loop gain*, a common function defined in control systems. At frequencies where the magnitude of  $G(f)$  is high, the residual strain  $s_{\text{res}}$  is smaller than the external strain  $s$ , and the control strain  $s_c$  is approximately equal to the external strain. When the magnitude of  $G(f)$  is small, the control strain  $s_c$  is small, and the residual strain is approximately equal to the external strain. In general, the magnitude of the open loop gain is high at frequencies below 100 Hz, to make the residual motion smaller than the linewidth of the optical cavities, keeping them near resonance.

The measured signal is

$$e(f) = C(f)s_{\text{res}}(f) = s(f)\frac{C(f)}{1 + G(f)}, \quad (1)$$

so the desired response function, used to calibrate the signal  $s(f) = R(f)e(f)$ , is

$$R(f) = \frac{1 + G(f)}{C(f)}. \quad (2)$$

### 3. Calibration methods of the actuation function

As we mentioned earlier, the calibration of the actuation function is critical to the whole process of reconstructing the function  $R(f)$ . The procedure involves several steps, starting with the laser wavelength ( $\lambda = 1064$  nm) as the length standard. Using only the beamsplitter and the input mirrors of the arm cavities, a simple Michelson loop signal is read at the antisymmetric port, and a feedback loop is closed acting on only one of the mirrors. Two general classes of methods are used to calibrate the actuation function to the desired input test mass, using either the error signal or the control signal of the Michelson loop [10]. If there is no feedback control, the mirrors' motion will produce a differential displacement function  $x(t) = L_x(t) - L_y(t)$ , and the sensor signal at the dark port is  $e(t) = S_0 \sin(4\pi x(t)/\lambda)$ . The power at the antisymmetric port is  $p(t) = P_0 \sin^2(2\pi x(t)/\lambda)$ . We can easily obtain the peak values  $S_0$  and  $P_0$  in volts, or counts of the signal that is read, by driving the mirrors to swing through full fringes.

If external disturbances are small enough, a mirror can be driven at a fixed slow frequency that sweeps through several fringes before turning back. The observed signals for power and sensor signal can then be fitted to the motion, and the known wavelength (1064 nm) can be used to calibrate the motion and thus the actuation function.

If the feedback loop is closed, the sign of the loop can be toggled to produce a dark or a bright output at the sensing photodiode. With high gain, the step produced when toggling the sign is an odd integer number of quarter-wavelengths  $\lambda/4$ , and in general is only  $\lambda/4$  or  $3\lambda/4$ . By repeating the procedure many times, measuring the control signal needed to move the mass each time, and taking differences of the consecutive signals, a calibration of the actuation can again be obtained (and the predicted quantization can be confirmed).

Alternatively, if the peak amplitude  $S_0$  is measured, when the loop is closed, the error signal near the null point is calibrated:  $k = de/dx|_{x=0} = S_0(4\pi/\lambda)$ , and  $e(t) = kx(t)$ . We then drive the mirror at different frequencies with a swept sine function, and measure the motion produced with the calibrated error signal. The advantage of this method is that we can measure the response at the frequencies in the gravitational wave band.

Having calibrated the actuation function on the input test masses with one or more of the methods described, we align an input test mass and the corresponding test mass at the end of the arm. We close a feedback loop on the resonant optical cavity of the single arm by actuating on the end test mass. We can then drive the calibrated input test mass with a

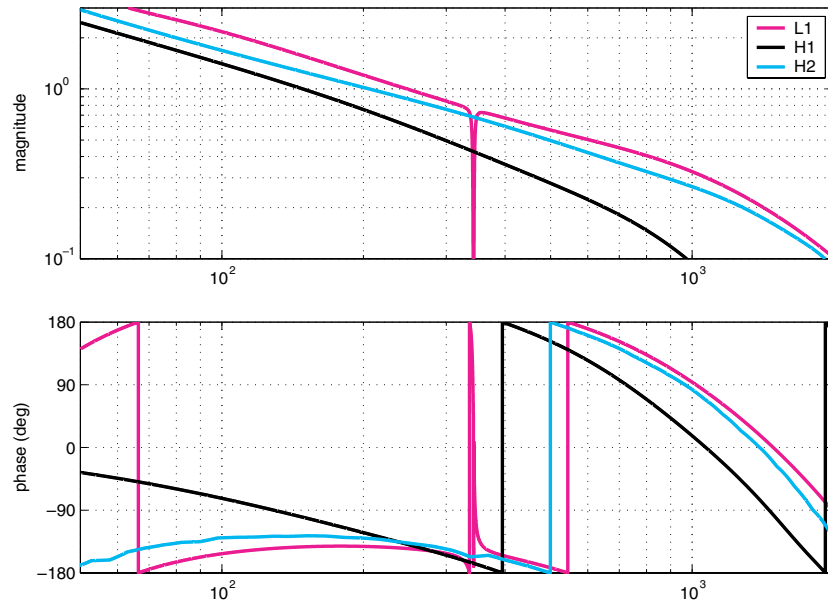


**Figure 2.** Open loop gains  $G(f)$  taken as reference for the S1 run. The curves shown are smoothed versions of the measurements (for H1 and H2), and the curve inferred from the model for the gain function (for L1). The notch in the L1 open loop gain was used to avoid ringing the violin modes of the suspended mirrors. The times for the reference measurements were Sep 06, 2002, 23:02 UTC (L1), Sep 04, 2002, 06:39 (H1) and Aug 29, 2002, 08:21 (H2).

sine wave of known amplitude; assuming the measurement is done at frequencies with high loop gains, we can infer the motion of the end test mass. Alternatively, we can calibrate the error signal of the feedback loop using a known drive to the input test mass, and thus infer the actuation on the end test mass at different frequencies, independently of the magnitude of open loop gain.

The measurements are reported as ‘DC gains’ of pendulum transfer functions for each mass, in metres/count. Calibrations obtained for S1 were 1.30 nm/count (ETMX, H2), 1.38 nm/count (ETMY, H2); 0.85 nm/count (ETMX, H1), 0.87 nm/count (ETMY, H1); 2.53 nm/count (ETMX, L1), and 2.67 nm/count (ETMY, L1). The differences are due to slightly different driving electronics between the two observatories, and to slight differences in electronic components, coils and magnets used for each mirror. The relative error in these measurements is  $\approx 8\%$ .

#### 4. Measurements of the feedback open loop gain

The open loop gain  $G(f)$  was measured directly several times during the S1 run. As expected, only the overall gain (determined by optical gains in the cavities, and thus alignment) was seen to change. We took one of these measurements as a reference measurement, which was then used as a starting point to track changes in gain during the run. A smoothed version of the reference measurements in the gravitational wave band (50 Hz–2000 Hz) is shown in figure 2. The three detectors had slightly different feedback filters, but all loops had a similar bandwidth (or control band): in the reference measurements, the unity gain frequencies were

**Table 1.** Calibration lines injected in the LIGO detectors during the S1 run.

Detector	Frequency (Hz)	Amplitude (m)	Amplitude (strain)
L1	51.3	$2.2 \times 10^{-14}$	$5.5 \times 10^{-18}$
L1	972.8	$3.8 \times 10^{-16}$	$9.5 \times 10^{-20}$
H1	37.25	$1.3 \times 10^{-12}$	$3.3 \times 10^{-16}$
H1	973.3	$6.4 \times 10^{-16}$	$1.6 \times 10^{-19}$
H2	37.75	$1.35 \times 10^{-13}$	$6.8 \times 10^{-17}$
H2	973.8	$8.1 \times 10^{-16}$	$4.1 \times 10^{-19}$

150 Hz (H1), 200 Hz (H2) and 250 Hz (L1). The overall gain and therefore the unity gain frequency changed during the S1 run, depending on the fluctuating optical gains. Using a model of the actuation and feedback filter functions, we can calculate the sensing function for the same reference times.

## 5. Use of calibration lines

Since it was recognized that the calibration changed considerably on a time scale of tens of minutes, we introduced calibration lines to track the changes in gains. This is a well-known technique, common in interferometric detectors [9]. Each detector had two calibration lines at different frequencies, one below the unity gain frequency and one near 1 kHz, where the loop gain was low. The sinusoidal excitations acted on the mirrors at the end of the X-arms of each detector. In the absence of a feedback loop, the excitations produced a sine wave of peak amplitude shown in table 1, clearly visible in the spectrum of the error signal  $e(f)$ . The low-frequency line is suppressed by the loop gain, so it appears smaller than the magnitudes shown in table 1, while the observed high-frequency line amplitude was very close to that presented in the same table.

The amplitudes of the lines in the spectrum were measured using a 1 min averaging time [11]. At the reference time when the open loop gain  $G_{\text{ref}}$  was measured, the amplitude of a calibration line injected with a known amplitude  $s_0$ , at a frequency  $f_{\text{cal}}$  in the error signal is given by equation (1):  $e_0(f_{\text{cal}}) = C_0(f_{\text{cal}})/(1 + G_0(f_{\text{cal}}))$ . The sensing function  $C_0$  can be calculated from the measured  $G_0$  and the modelled actuation and feedback filter functions, which have fixed gains:  $C_0 = G_0/(AD)$ .

Assuming the sensing function fluctuations (and therefore those of the open loop gain) can be parametrized by an overall multiplicative factor  $\alpha(t)$ , the amplitude of the calibration lines at any time during S1 will be

$$e(f_{\text{cal}}, t) = \alpha(t) \frac{C_0(f_{\text{cal}})}{1 + \alpha(t)G_0(f_{\text{cal}})} = e_0(f_{\text{cal}}) \alpha \frac{1 + G_0(f_{\text{cal}})}{1 + \alpha(t)G_0(f_{\text{cal}})}.$$

From the ratio of the measured amplitude  $e(f_{\text{cal}}, t)$  and the reference amplitude  $e_0(f_{\text{cal}})$ , we get the amplitude of the function  $\alpha(t)$ .

The feedback filter  $D$  was changed a few times during S1 in L1, to tune the feedback filters for optimal operation with changing amounts of light on the photodiode. If we consider  $D$  changing by a known ratio  $\beta$  from its reference value and the sensing function changing by the ratio  $\alpha$  considered above, then the open loop gain will change by a factor  $\alpha\beta$  and the

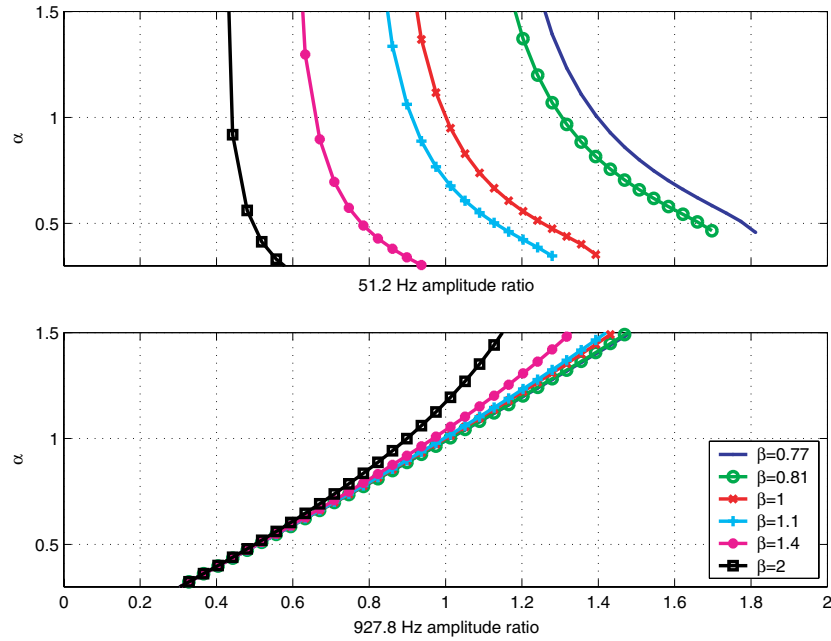


**Figure 3.** The inferred value of  $\alpha$  from the measured ratio of the amplitude of the calibration lines at any given time, to the amplitude of the same line at the reference time for L1, Sep 06, 2002, 23:02 UTC. Since there were several values of gains used for the feedback filter function  $D(f)$ , we have one curve for each  $\beta$ .

measured line amplitude will be

$$e(f_{\text{cal}}, t) = \alpha(t) \frac{C_0(f_{\text{cal}})}{1 + \alpha(t)\beta G_0(f_{\text{cal}})} = e_0(f_{\text{cal}}) \alpha \frac{1 + G_0(f_{\text{cal}})}{1 + \alpha(t)\beta G_0(f_{\text{cal}})}.$$

The graphs used to deduce the value of  $\alpha(t)$  from the measured ratios  $e(f_{\text{cal}}, t)/e_0(f_{\text{cal}})$  in the L1 detector, for all values of  $\beta$  used during S1, are shown in figure 3. Since the loop gain at the high-frequency line is small ( $\approx 0.3$ ), the amplitude of the line is approximately linearly dependent on the value of  $\alpha$ ; while the amplitude of the low-frequency line, where the loop gain is high ( $\approx 4$ ), has a steep, nonlinear dependence on the value of  $\alpha$ . For this reason, we used the high-frequency line to derive our estimate of  $\alpha$ , and only used the lower frequency line as a consistency check.

There is only a finite possible range for the product  $\alpha\beta$  that makes the loop stable: if the gain drifts too high or too low, the feedback loop will become unstable and the detector will not be operational. For example at L1 this range is  $0.4 \leq \alpha\beta \leq 1.4$ .

Once we know the value of  $\alpha$  (and  $\beta$ ) at any given time, we can deduce the response function, from equation (2):

$$R(f, t) = \frac{1 + \alpha(t)\beta G_0(f)}{\alpha(t)C_0(f)}. \quad (3)$$

In general this will not be a simple scaling of the the response function at the reference time. The changes can be very significant, as shown in figure 4, where the reference calibration for

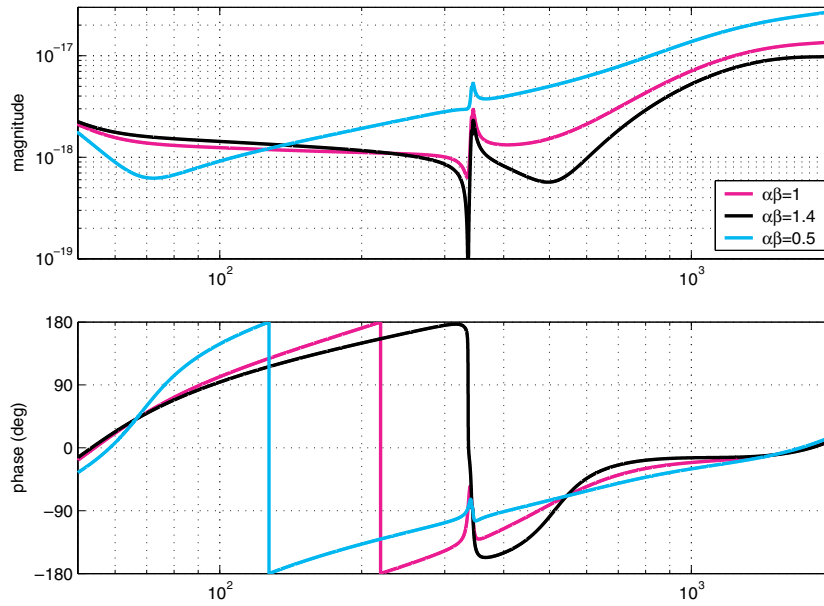


**Figure 4.** Response function  $R_0(f)$  for L1 at reference time Sep 06, 2002, 23:02 UTC, when  $\alpha\beta = 1$ , and response functions for extreme values of the open loop gain scale  $\alpha\beta = 0.5$  and  $1.4$ . These two latter curves should be taken as an envelope of possible response functions during S1. The values of  $\alpha\beta$  for L1 had a median of  $0.76$ , and were usually between  $0.5$  and  $1.0$ .

L1 is shown, together with the calibrations obtained for gains close to maximum and minimum values of the product  $\alpha\beta$ .

## 6. Calibration results and stability during S1

We took as reference functions the best measurements of loop gains during S1; the corresponding reference calibrations are shown in figure 5. This response is then recalculated using equation (3) for every minute of data during S1 when the interferometers were in operation and when an estimation of  $\alpha$  was available.

The measured gain factor  $\alpha\beta$  as a function of time is shown in figure 6 for the three detectors. The breaks in the plot are due to the fact that the interferometers were not in continuous operation for more than a few hours at a time. The duty cycle varied between 42% (for L1) to 73% (for H2). There is a significant drift, even within a continuous segment when the detector is in operation, due to fluctuations in alignment. These fluctuations will ultimately be controlled by angular control feedback loops, which were only partially commissioned at the time of S1. The fluctuations are not random, and the distribution of values is not Gaussian, as shown in the histograms of all values, in figure 7.

There is also some random scatter due to the statistical error in the estimation of the line amplitude. If we take the difference of consecutive measurements of the line amplitude, we see that its distribution is now Gaussian, which is more typical of statistical errors in the amplitude spectral estimate than of alignment fluctuations with a 1 min time scale. We can use the width of these distributions to assign an error to any single estimate of  $\alpha(t)$ . These errors vary

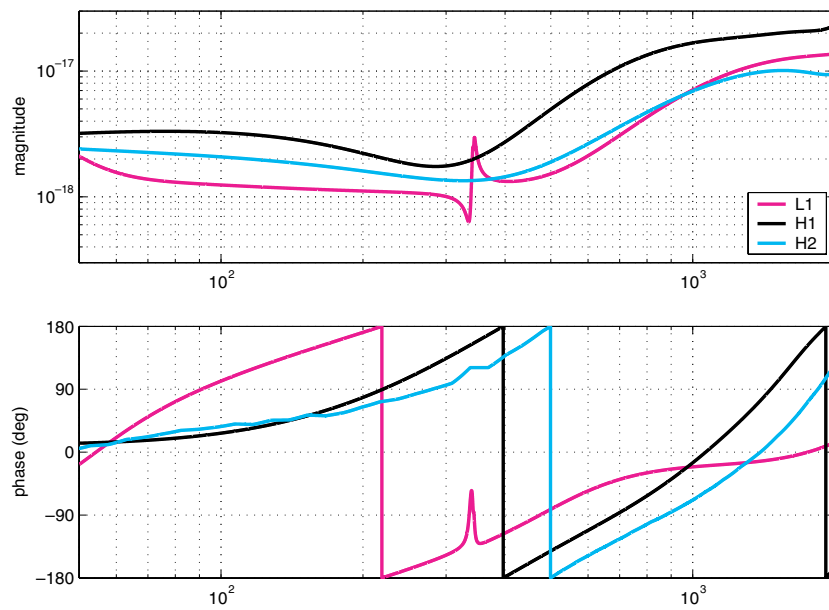


**Figure 5.** Response functions  $R(f)$  for the three LIGO detectors at the reference times, derived from open loop gains shown in figure 2.

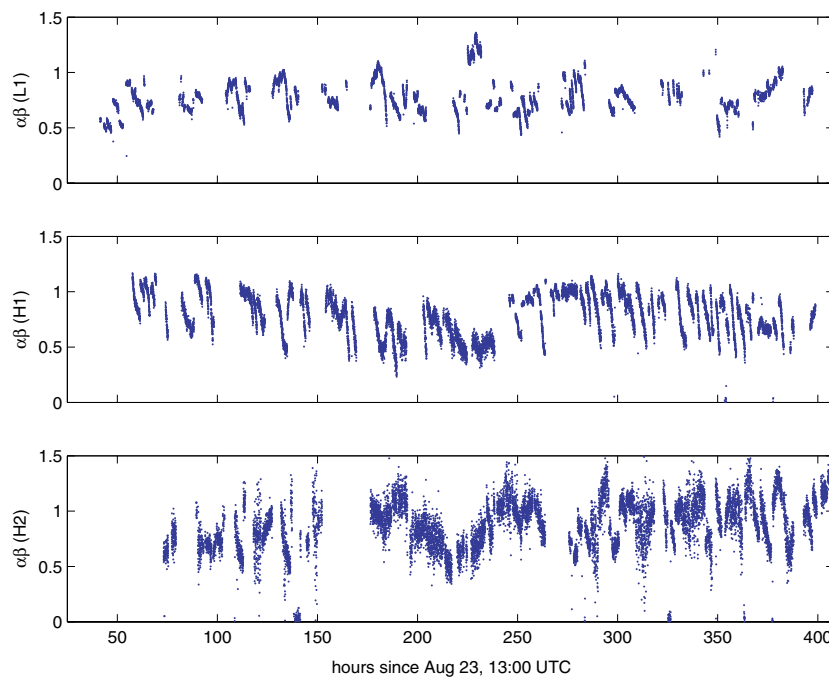


**Figure 6.** Open loop gain ratio  $\alpha\beta$  to the reference times during S1 times when data were available for data analysis. The first day was dedicated to calibration, so it does not include available data.

between 2% (for L1) to 7% (for H2), and are mostly dependent on the signal-to-noise ratio of the calibration lines. The weight of the statistical error in  $\alpha$  into the response function  $R(f)$

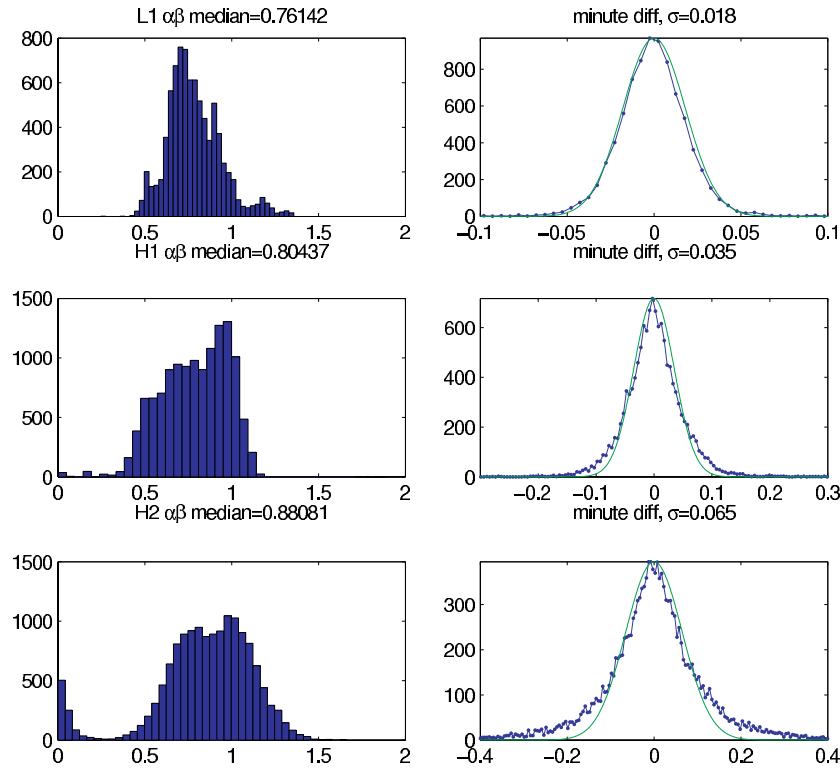


**Figure 7.** The left-hand side shows the histogram of the values  $\alpha\beta$  in the three detectors. The distributions are not Gaussian, indicating systematic variations due to alignment fluctuations. On the right-hand side, we plot the histogram of the difference between consecutive values. These values are better approximated by Gaussian distributions, representing the statistical error in the estimate of  $\alpha\beta$  from the amplitude of calibration lines.

is  $1/(1 + \alpha G_0(f))$ , which has a magnitude smaller than one, so the error in the magnitude of the response function due to the statistical error in  $\alpha$  is never larger than 7%.

## 7. Conclusions

We have described the method used for calibrating the LIGO detectors during the First Science Run of the LIGO Science Collaboration. We also presented the calibrations used as a reference, and the fluctuations of the sensitivity of the detectors during the run. A second scientific run (S2) has already occurred at the time of writing this paper, and the same techniques were applied. An automated calibrator, developed initially at the Hanford Observatory during S1, was used at all three detectors during S2. The 4 km LIGO detector at the Hanford Observatory had a more advanced alignment control system, which resulted in a more stable calibration, as predicted by the models described here. In the future, we expect to use a different actuator (using radiation pressure on a mirror from an auxiliary laser source), to more precisely determine the actuation function. At present this determination is the largest source of uncertainty in the calibration. For the S1 calibration we estimate an error of less than 10% in magnitude and less than  $10^\circ$  in phase for the response function. This calibration was used by many different groups searching for different kinds of gravitational wave sources. As data

analysis methods improve, their results will become more sensitive to errors in the detectors' calibration. The experience gained in calibrating the S1 data provided the opportunity for a careful analysis of stability and errors that we are already using to improve measurements and methods.

### Acknowledgments

We acknowledge the support of the US National Science Foundation under Cooperative Agreement no PHY-0107417, and individual grant no PHY-0135389. We also gratefully acknowledge the support of the LIGO Science Collaboration and the LIGO Laboratory, who conducted the First Science Run.

### References

- [1] Abramovici A *et al* 1992 *Science* **256** 325
- [2] Barish B and Weiss R 1999 *Phys. Today* **52** 44
- [3] Willke *et al* 2002 *Class. Quantum Grav.* **19** 1377
- [4] Acernese F *et al* 2002 *Class. Quantum Grav.* **19** 1421
- [5] Tagoshi H *et al* 2001 *Phys. Rev. D* **63** 062001
- [6] Saulson P R 1994 *Fundamentals of Interferometric Gravitational Wave Detectors* (Singapore: World Scientific)
- [7] Fritschel P, Bork R, González G, Mavalvala N, Ouimette D, Rong H, Sigg D and Zucker M 2001 *Appl. Opt.* **40** 4988
- [8] Fritschel P, González G, Mavalvala N, Shoemaker D, Sigg D and Zucker M 1998 *Appl. Opt.* **37** 6734
- [9] Telada S *et al* 1999 *Proc. 2nd TAMA Int. Workshop on Gravitational Wave Detection* (Tokyo: Universal Academy Press) pp 129–36
- [10] Adhikari R, Evans M, Landry M, Marka S, Matone L and Yamamoto H 2002 *LIGO Technical Document T020141-00-D* webpage <http://admbdbsrv.ligo.caltech.edu/dcc/>
- [11] Klimentko S, Mitselmakher G, Sazonov A, Daw E and Castiglione J Line Monitor *LIGO Technical document LIGO-T010125-01-D*